Collision-Free Lifetimes of SO($B^3\Sigma^-$, $v' = 0$, 1, and 2) and Vibrational Level Dependence of Deactivation by He

Katsuyoshi Yamasaki,* Fumikazu Taketani, Sachie Tomita, Kazuyuki Sugiura, and Ikuo Tokue

Department of Chemistry, Niigata University, Ikarashi, Niigata 950-2181, Japan

Received: October 4, 2002; In Final Form: January 16, 2003

Collision-free lifetimes and deactivation rate constants of SO($B^3\Sigma^-$, $v' = 0$, 1, and 2) by collisions with He have been determined. SO($X^3\Sigma^-$) was generated in the photolysis of SO_2 at 193 nm (ArF laser) and excited to a single rovibrational level of $B^3\Sigma^-$ with a pulsed ultraviolet laser. We recorded dispersed fluorescence spectra, and found that 0−12 (350.8 nm), 1−14 (368.5 nm), and 2−17 (401.2 nm) bands are suitable for detecting fluorescence from single vibrational level of interest. Time profiles of wavelength-resolved fluorescence were recorded at various buffer gas pressures (5−165 Torr of He). Deconvolution by the integrated phase plane method derives apparent fluorescence lifetime at a given pressure. Total pressure dependence of fluorescence decay rates leads to collision-free lifetimes and rate constants for deactivation of SO($B^3\Sigma^-$, $v' = 0$, 1, and 2) by collisions with He. Lifetimes of SO($B^3\Sigma^-$) have been determined to be (28 ± 2) ns ($v' = 0$), (30 ± 3) ns ($v' = 1$), and (27 ± 4) ns ($v' = 2$). Rate coefficients for deactivation of SO($B^3\Sigma^-$) by He have been obtained to be (6.3 ± 0.3) × 10^{-12}, (3.9 ± 0.2) × 10^{-11}, and (1.3 ± 0.2) × 10^{-10} in units of cm^3 $molecule^{-1}$ s^{-1} for $v' = 0$, 1, and 2, respectively. To the best of our knowledge, deactivation rate constants for $v' = 0$ and 1 of SO($B^3\Sigma^-$) are measured for the first time in the present study. The large rate coefficient of deactivation by He and vibrational level dependence is explained by predissociation via the $C^3\Pi$ state.

Introduction

The SO radical has been proposed as a medium for a widely tunable ultraviolet laser.[1−6] There are two electronically excited states, $A^3\Pi$ and $B^3\Sigma^-$, lying close to the first dissociation limit to S(^{3}P) + O(^{3}P), and their internuclear distances, 0.161 nm ($A^3\Pi$) and 0.1775 nm ($B^3\Sigma^-$), are longer than that of the ground-state $X^3\Sigma^-$ (0.1481 nm).[7] Therefore, the Franck−Condon envelope of v'' progression stretches over a wide range of wavelength and offers an advantage for realizing a ultraviolet tunable laser. The energy difference between these states, $\Delta E = 3320$ cm^{-1}, is small compared to their excitation energies, 38 306 and 41 639 cm^{-1} for $A^3\Pi$ and $B^3\Sigma^-$, respectively.[7,8] The two states, however, have totally different photochemical properties. For example, the radiative lifetime of the lowest vibrational level of $A^3\Pi$ is about 35−39 μs,[2,5,9] and that of $B^3\Sigma^-$ is 17.3 ns.[10] In contrast to $A^3\Pi$, rotational levels higher than $N' = 65$, 53, 37, and 10 of $v' = 0$, 1, 2, and 3 of $B^3\Sigma^-$ undergo efficient predissociation to S(^{3}P) + O(^{3}P) by way of the $C^3\Pi$ state.[8,11]

Smith[10] measured radiative lifetimes of SO($B^3\Sigma^-$) by phase shift techniques, and reported lifetimes to be $\tau_{v'=0} = 17.3 \pm 3.3$ ns, $\tau_{v'=1} = 16.6 \pm 3.3$ ns, and $\tau_{v'=2} = 16.2 \pm 3.3$ ns. Stuart et al.[12] have also measured radiative lifetimes of SO($B^3\Sigma^-$, $v' = 1$ and 2) by pulsed laser excitation with continuously tunable KrF laser and found no rotational level dependence of the lifetimes of $v' = 1$. In contrast to the $v' = 1$ case, the lifetimes of $v' = 2$ are strongly dependent on rotational levels because of perturbation by the $C^3\Pi$ and/or $A^3\Pi$ states, ranging from 28 to 91 ns. Stuart et al. did not measure the lifetime of $v' = 0$, because the tunable range of their laser was too narrow to excite $0-v''$ bands in the $B^3\Sigma^- - X^3\Sigma^-$ system. There is still a large discrepancy between the previously reported lifetimes of SO($B^3\Sigma^-$).

In the present study, SO($X^3\Sigma^-$) was generated by the photolysis of SO_2/He mixture at 193 nm and excited to a single vibrational level of $B^3\Sigma^-$ ($v' = 0$, 1, and 2) with a tunable laser. Time profiles of the fluorescence intensity were recorded at a wide range of buffer gas pressures (5−165 Torr of He). Careful deconvolution analysis was made using the integrated phase plane method,[13] and radiative lifetimes and deactivation rate constants for $v' = 0$, 1 and 2 of $B^3\Sigma^-$ have been determined from fluorescence decay rates as a function of buffer gas pressures.

Experimental Section

A schematic diagram of the experimental apparatus is shown in Figure 1. SO_2 was photolyzed at 193 nm with an ArF excimer laser (Lambda Physik LEXtra50, 19 Hz) at 298 ± 2 K, and SO($X^3\Sigma^-$) was generated. Vibrational levels of SO($B^3\Sigma^-$, $v' = 0-2$) were excited via the 0−2 (256.16 nm), 1−1 (245.14 nm), and 2−2 (248.30 nm) bands in the $B^3\Sigma^- - X^3\Sigma^-$ system with a Nd^{3+}:YAG laser (Spectron SL803) pumped dye laser (Lambda Physik LPD3002 with LD489/MeOH). Time delays between the photolysis (ArF) and excitation (dye) laser were 20 μs in all measurements. Excited rotational lines are assigned to $P_{11}(17)/P_{33}(17)$ lines for the 0−2 band and $P_{11}(15)/P_{33}(15)$ for the 1−1 band using previously reported spectroscopic data.[8,11,14−17] Labels for rotational lines such as $P_{11}(17)$ are defined to be $\Delta N_{ij}(N'')$, where N is a quantum number of total angular momentum apart from spin and the subscripts i and j represent spin sublevels of upper and lower levels, respectively. It is difficult to identify the excited rotational levels of the 2−2 band,

* To whom correspondence should be addressed. Fax: +81-25-262-7530. E-mail: yam@scux.sc.niigata-u.ac.jp.

10.1021/jp027129a CCC: $25.00
Published on Web 03/15/2003

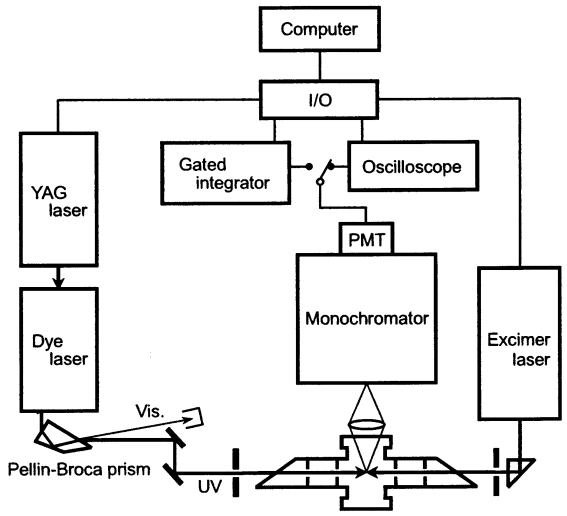

Figure 1. Schematic diagram of the experimental apparatus. Light (355 nm) from the YAG laser excites the dye laser (LD489 dye) at a repetition rate of 19 Hz. Ultraviolet output is separated from the fundamental (visible) beam with the Pellin-Broca prism. The PMT is terminated with a 1 kΩ load resistor to observe fluorescence spectra, and the output from the PMT is fed into the gated integrator. A 50 Ω load resistor is used to record time-resolved fluorescence profiles, and the output of the PMT is transferred to the oscilloscope.

because $v' = 2$ of $B^3\Sigma^-$ is highly perturbed,[8,12,16] and no decisive rotational assignment has been reported. The rotational line of the 2−2 band excited in the present study is assignable to $R(20)$ based on the tentative numbering given by Stuart et al.[12] SO($A^3\Pi - X^3\Sigma^-$) transitions, which can appear over the almost identical wavelength range with the $B^3\Sigma^- - X^3\Sigma^-$ system,[1−5,7,9,18−26] does not disturb the present experiments, because the effective absorption cross section of the $A^3\Pi - X^3\Sigma^-$ system, 6.9×10^{-17} cm^2, is less than 3% of that of $B^3\Sigma^- - X^3\Sigma^-$ transition, 2.5×10^{-15} cm^2.[12]

Fluorescence was collected with a quartz lens ($f = 80$ mm), focused on the entrance slit of a monochromator (JEOL JSG-125S, $f = 125$ cm, $\Delta\lambda$(fwhm) = 3 nm), and detected with a photomultiplier tube (Hamamatsu R928). All of the rotational lines of a single vibrational band are included in the spectral bandwidth of the monochromator. Wavelength dependence of the sensitivity of photo detection system was calibrated with a super-quiet Xe lamp (Hamamatsu L2273). When dispersed fluorescence spectra were recorded, the PMT was terminated with a 1 kΩ load resistor, and the signal averaged with a gated integrator (Stanford SR-250) was stored on a disk of a PC. When fluorescence decay curves were observed, on the other hand, the resistor was set at 50 Ω, and the output from the PMT was fed into a digital oscilloscope (Tektronix TDS420A, time resolution: 20 ps), and the signals from 10000 laser pulses were averaged. At least three profiles were recorded and averaged to obtain an adequate signal-to-noise ratio.

The wavelengths of $v'-v''$ bands are close to those of $(v' + 2)-(v'' + 1)$ bands, because vibrational quantum energy of $B^3\Sigma^-$ is about a half of that of $X^3\Sigma^-$: $\omega_e' = 622.5$ and $\omega_e'' = 1150.695$ cm^{-1}.[8] Fortunately, the transition wavelength of the rotational line used for exciting the 2−2 band was shorter than that of the head of the 0−1 band, and consequently, none of the rotational lines of the 0−1 band are excited simultaneously with the 2−2 band. Rotational lines of the 2−3 and 3−2 bands, on the other hand, partly overlap with those of the 0−2 and 1−1 bands, respectively. However, dispersion enables us to observe fluorescence from a single vibrational level of interest. The wavelength of the monochromator was tuned to the 0−12 (350.8 nm), 1−14 (368.5 nm), and 2−17 (401.2 nm) bands for monitoring fluorescence from $v' = 0$, 1, and 2, respectively. As shown in the later section, dispersed fluorescence via the three bands detected with 3 nm of resolution does not overlap with any vibrational band. Fluorescence excited via the 4−3 and 5−3 bands, whose rotational lines might overlap with the 2−2 and 1−1 bands, respectively, are negligible, because vibrational levels higher than $v' = 3$ are nonfluorescent because of efficient predissociation[8,11] and because nascent populations of SO($X^3\Sigma^-$, $v'' \geq 3$) generated in the photolysis of SO_2 at 193 nm is very small.[27−32]

Assuming the SO yield to be near unity,[33,34] the approximate concentration of initially prepared SO can be estimated to be about 5×10^{11} cm^{-3} from the energy density of the photolysis laser at the entrance window of the reaction cell (≤1 mJ cm^{-2}), photoabsorption cross section of SO_2: $\sigma(193\text{ nm}) = 7.9 \times 10^{-18}$ cm^2[12] and 6.3×10^{-18} cm^2,[35] and a typical pressure of SO_2 (3 mTorr).

Photoabsorption cross sections of SO_2 at the wavelengths of excitation laser ($\lambda \approx 250$ nm) have been reported to be 1×10^{-19} cm^2.[12,35,36] This value is smaller than that of SO by about 25 000. Concentration ratio $[SO_2]/[SO]$ is about 200, and thus, the number of excited SO_2 is less than 1% of that of SO. Fluorescence yield of SO_2 excited at $\lambda > 240$ nm is very small,[37] and no fluorescence from SO_2 was actually observed upon excitation at $\lambda > 239$ nm in the present study.

The flow rates of all of the sample gases were controlled with calibrated mass flow controllers (Tylan FC-260KZ and STEC SEC-400 mark3) and mass flow sensors (KOFLOC 3810). Linear flow velocity was 10 cm s^{-1} irrespective of buffer gas pressures. Total pressure (He buffer) was monitored with a capacitance manometer (Baratron 122A). The total pressure measurement together with the mole fractions as measured by the flow controllers gave the partial pressures of the reagents. SO_2 (Nihon-Sanso, > 99.9%) and He (Nihon-Sanso, 99.9999%) were used without further purification.

Results and Discussion

Dispersed Fluorescence Spectra and Time Dependent Profiles of SO($B^3\Sigma^- - X^3\Sigma^-$). Figure 2 shows dispersed fluorescence spectra recorded at 5 Torr of He buffer gas. All of the peaks are assigned to the v'' progression of SO($B^3\Sigma^- - X^3\Sigma^-$), and the intensity distributions clearly show Franck−Condon envelopes.[38,39] The wavelengths of vibrational bands were calculated using vibrational constants reported by Clerbaux and Colin.[8] Faint peaks at 283, 292, and 358 nm in Figure 2a are assigned to the 1−6, 1−7, and 1−13 bands, indicating that vibrational relaxation occurs by collisions of 5 Torr of He, although it is inefficient. Fortunately, the 0−12, 1−14, and 2−17 bands, which are indicated with the arrows, do not overlap with any other peaks. Therefore, fluorescence from a single vibrational level can be detected using these bands, even if vibrational relaxation populates different vibrational levels from those initially prepared.

Figure 3 shows time-resolved fluorescence following excitation to $v' = 0$, 1, and 2 at 50 Torr of He. The excitation laser pulse, whose duration is 15.5 ns (fwhm), was recorded with the monochromator tuned to the wavelength of the excitation laser. Simple semilogarithmic analysis is not applicable to determine apparent fluorescence decay rates, because the duration of the excitation laser is not sufficiently small compared to the decay period of fluorescence. Therefore, deconvolution of observed time profiles using the excitation laser pulse must be made to derive fluorescence decay rates. Here, the procedures for the actual analysis are described.

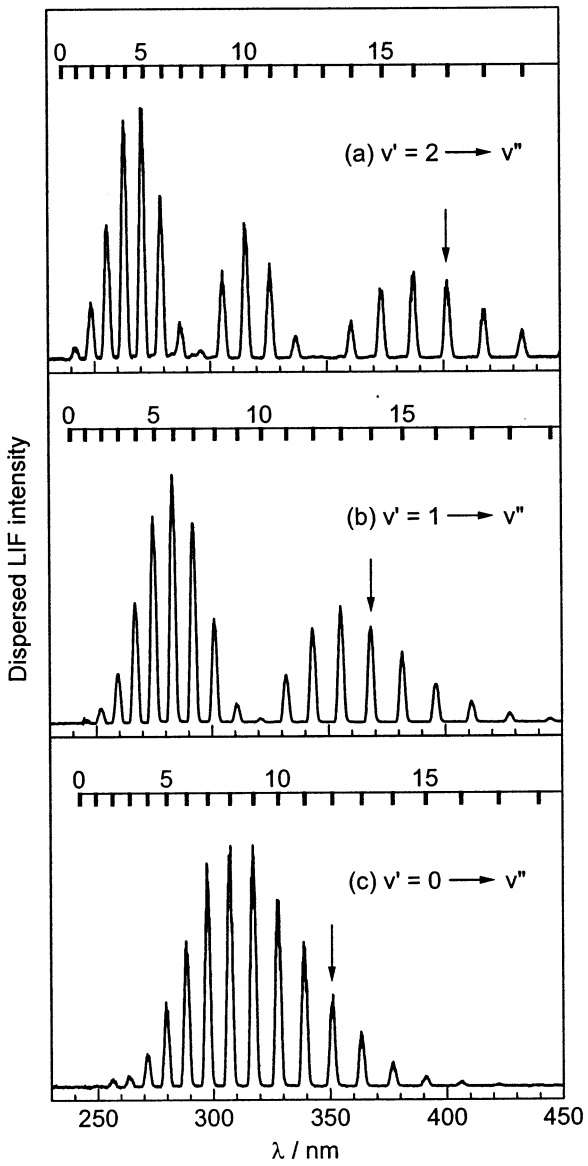

Figure 2. Dispersed fluorescence spectra of $SO(B^3\Sigma^- \rightarrow X^3\Sigma^-)$. Excitation wavelengths are (a) 248.30 ($R(20)$ of the 2−2 band), (b) 245.14 ($P_{11}(15)/P_{33}(15)$ of the 1−1 band), and (c) 256.16 nm ($P_{11}(17)/P_{33}(17)$ of the 0−2 band). The labels of rotational lines are defined to be $\Delta N_{ij}(N'')$, where N is the quantum number of total angular momentum apart from spin and the subscripts i and j represent spin sublevels of upper and lower states. $P_{SO_2} = 3$ mTorr, $P_{total}(He) = 5$ Torr. $SO(X^3\Sigma^-)$ is generated by the photolysis of SO_2 at 193 nm, and the delay times between the photolysis and excitation laser are 20 μs. The 0−12, 1−14, and 2−17 bands, indicated with the arrows, are monitored to record time profiles of fluorescence.

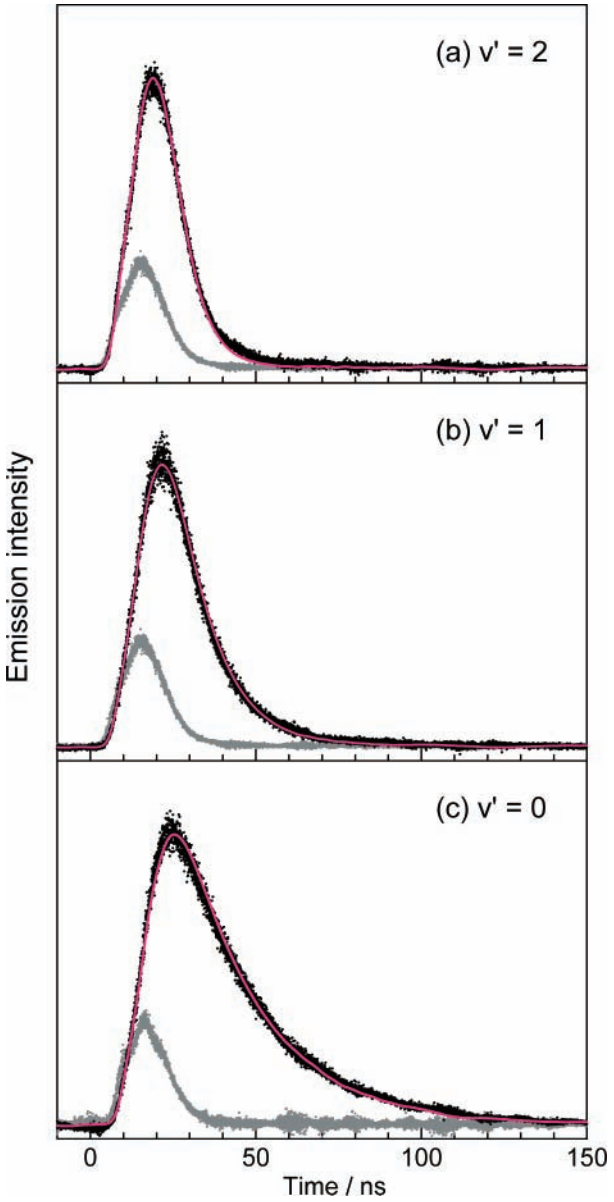

Figure 3. Time profiles of fluorescence of $SO(B^3\Sigma^- \rightarrow X^3\Sigma^-)$ following excitation to a single rovibronic level. Excitation wavelengths are identical with those of Figure 2. Fluorescence was detected at (a) 350.8 (0−12 band), (b) 368.5 (1−14), and (c) 401.2 nm (2−17). $P_{SO_2} = 3$ mTorr, $P_{total}(He) = 50$ Torr. The large signals (black dots) represent fluorescence signals $I(t)$, the small signals (gray dots) are the time profiles of excitation laser $L(t)$, and the red lines show convoluted signals calculated by eq 10 with the following overall decay rates (k): (a) 2.33×10^8 (4.29), (b) 9.80×10^7 (10.21), and (c) 4.57×10^7 s^{-1} (21.86 ns).

Possible fates of an excited single vibrational level of $SO(B^3\Sigma^-, v')$ are represented by the following scheme:

$$SO(X,v) + h\nu \xrightarrow{E(t)} SO(B,v') \quad (1)$$

$$SO(B,v') \xrightarrow{k_r} SO(X,v'') + h\nu' \quad (2)$$

$$SO(B,v') + He \xrightarrow{k_v} SO(B,v'-\Delta v) + He \qquad (v' \geq 1) \quad (3)$$

$$SO(X,v') + He \xrightarrow{k_Q} SO(X,v'') + He \text{ or } S + O + He \quad (4)$$

where $E(t)$ is a time-dependent rate of excitation in units of molecule cm^{-3} s^{-1}, and k_r, k_v, and k_Q are rate constants for radiative decay, vibrational relaxation, and quenching, respectively. Radiative lifetime τ_r is defined by reciprocal radiative decay: $\tau_r = 1/k_r$. Rate constants for upward vibrational relaxation ($\Delta v < 0$) are estimated to be less than 5% of those for downward relaxation at 298 K based on the principle of detailed balance and vibrational quantum energy of $B^3\Sigma^-$: 630 cm^{-1}.[8] The collision-free lifetime of $SO(B^3\Sigma^-)$ is at longest 100 ns in the present study.[10,12] Assuming the gas kinetic collision rate coefficient to be 5×10^{-10} cm^3 $molecule^{-1}$ s^{-1} at 298 K, the mean free time of collisions between $SO(B^3\Sigma^-)$ and SO_2 (3 mTorr) is about 20 μs. Therefore, the probability of collision of $SO(B^3\Sigma^-)$ with SO_2 is less than 5×10^{-3}, and there is no effect of 3 mTorr of SO_2 on the decay of $SO(B^3\Sigma^-)$.

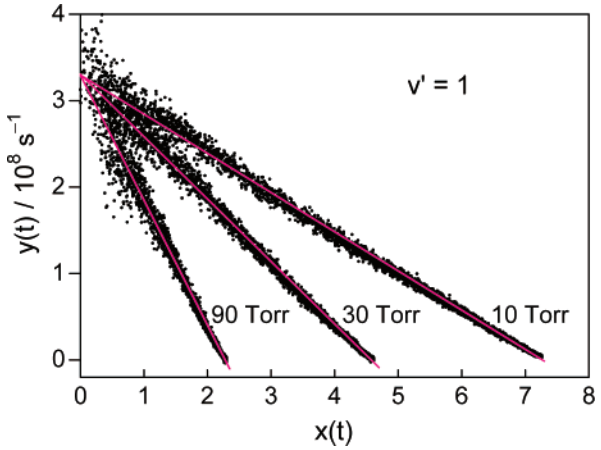

Figure 4. Integrated phase plane plots of the fluorescence from SO($B^3\Sigma^-$, $v' = 1$) excited at 245.14 nm (1−1 band) and observed at 368.5 nm (1−14 band) at different total pressures. Partial pressure of SO_2 was 3 mTorr. The ordinates $y(t)$ and abscissa $x(t)$ are defined by eqs 8 and 9 in the text. The red lines denote the results of linear regression analysis, giving apparent first-order decay rates of excited states.

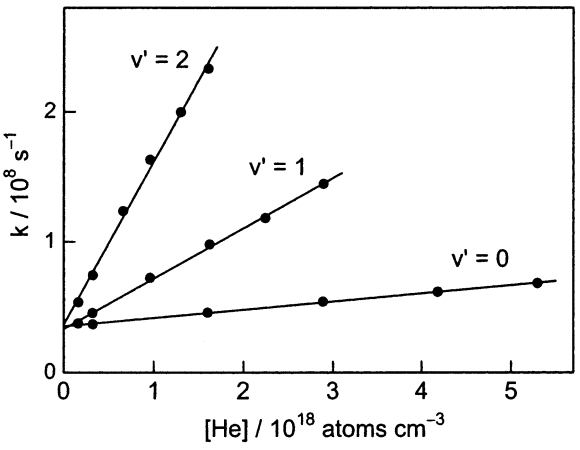

Figure 5. Total pressure dependence of apparent first-order decay rate constants. The ordinate k represents first-order decay rate constant defined by $k_r + (k_v + k_Q)$[He] (eqs 2−4). The intercepts of the plots correspond to collision-free lifetimes of the excited level, and the slopes give deactivation rate constants of SO($B^3\Sigma^-$, v') by He. Deactivation of $v' = 1$ and 2 are governed by vibrational relaxation (k_v) and quenching (k_Q); $k_v/(k_v + k_Q)$ are about 0.02 ($v' = 1$) and 0.08 ($v' = 2$).

Rate equation for [SO(B, v')]

$$\frac{d[SO(B, v')]}{dt} = E(t) - \{k_r + (k_v + k_Q)[He]\}[SO(B,v')] \quad (5)$$

can be transformed to be

$$I(t) = C\int_0^t L(t')\,dt' - k\int_0^t I(t')\,dt' \quad (6)$$

where the lower limits of integrations are defined to be the initial time of irradiation of the excitation laser. Time profiles of fluorescence intensity $I(t)$ and excitation laser pulse $L(t)$ are in proportion to [SO(B, v')] and $E(t)$: $I(t) = C_1$[SO(B, v')] and $L(t) = C_2E(t)$, where C_1 and C_2 are proportionality constants. C is defined to be C_1/C_2, and k ($= k_r + (k_v + k_Q)$[He]) is an apparent first-order decay rate at a given He pressure. After dividing both sides by integrated $L(t)$, the following equation is obtained:

$$y(t) = -kx(t) + C \quad (7)$$

where

$$y(t) = I(t)/\int_0^t L(t')\,dt' \quad (8)$$

$$x(t) = \int_0^t I(t')\,dt'/\int_0^t L(t')\,dt' \quad (9)$$

Therefore, a plot of $y(t)$ versus $x(t)$, which is called a phase plane (PP) plot,[13] must be linear. Figure 4 shows typical PP plots whose slopes give apparent first-order decay rates. It should be noted that the intervals of data points along abscissa in Figure 4 are not constant, because the values of $x(t)$ do not grow regularly with time. The density of points is higher at larger values of $x(t)$ in the present case, and as a consequence, scattering of data points at small values of $x(t)$ hardly affects the slopes (red lines) given by regression analysis. All of the time profiles of fluorescence recorded at different total pressures were analyzed in the same way.

We calculated convolution integrals to confirm whether the values of apparent decay rates determined by the PP plots are correct. Pseudo-first-order conditions are satisfied ([He]/[SO(B, v')] $\geq 10^5$), and consequently, decay of a single vibrational level SO(B, v') by processes 2, 3, and 4 is represented by a single exponential form: $\exp(-kt)$. This is a response function of SO(B, v') to an impulsive photoexcitation. As can be seen in Figure 3, the actual excitation laser is not an infinitesimal pulse but has a finite duration whose time profile is given by $L(t)$. Accordingly, the observed time-dependent fluorescence intensity is given by the following convolution integral:[13]

$$I(t) = C\int_0^t L(t')e^{-k(t-t')}\,dt' \quad (10)$$

where C and k have already been determined by the analysis using eq 7. Calculated $I(t)$ from $L(t)$ using eq 10 are also shown in Figure 3 with red lines. All the observed fluorescence profiles over the whole temporal range are well reproduced. The facts indicate that the scheme given by eqs 1−4 represent actual events induced by laser excitation, and that fluorescence decay rates obtained by the PP plots are reliable.

TABLE 1: Radiative Lifetimes SO($B^3\Sigma^-$, $v' = 0$, 1, and 2) and Rate Constants for Deactivation by He

v'	τ/ns	k^a/cm^3 molecule^{-1} s^{-1}	refs
0	17.3 ± 3.3		10
	28 ± 2[b]	(6.3 ± 0.3[c]) × 10^{-12}[b]	this work
1	16.6 ± 3.3		10
	33.3 ± 3[d]		12
	30 ± 3[e]	(3.9 ± 0.2[c]) × 10^{-11}[e]	this work
	32 ± 2[f]	(3.6 ± 0.2[c]) × 10^{-11}[f]	this work
2	16.2 ± 3.3		10
	31.3[d]	(1.3 ± 0.3) × 10^{-10}[g]	12
	27 ± 4[d]	(1.3 ± 0.2[c]) × 10^{-10}[d]	this work

[a] Collisional quenching for $v' = 0$, and the sum of quenching and vibrational relaxation for $v' = 1$ and 2. [b] $N' = 16$. [c] Quoted errors are 2σ. [d] $N' = 21$. [e] $N' = 14$. [f] $N' = 30$. [g] $N' = 15$.

Collision-Free Lifetimes of SO($B^3\Sigma^-$, $v' = 0$, 1, and 2). Plots of the first-order fluorescence decay rates versus He pressures are shown in Figure 5. Radiative lifetimes determined from the intercepts are (28 ± 2), (30 ± 3), and (27 ± 4) ns for $v' = 0$, 1, and 2, respectively, and listed in Table 1 along with previously reported values. The fact that collision-free lifetimes of SO($B^3\Sigma^-$) are independent of vibrational levels is in contrast to SO($A^3\Pi$) which shows a large variation with vibrational quantum number: 35−39 μs of $v' = 0$ and 9.8 μs of $v' = 6$.[1,2,5,9,12]

Smith[10] has employed a phase shift technique to measure the radiative lifetimes. The discrepancy of their lifetimes is partly due to the incorrect assignment of the spectrum. Stuart et al.[12] excited blended $R_{11}(20)/R_{33}(20)$ rotational lines of the 1−2 band at 100 mTorr of SO_2 and no buffer gas, determining the radiative lifetime to be 33.3 ± 3 ns. Their value is in good agreement with ours (30 ± 3 ns) despite different rotational levels and pressures of SO_2. We have also measured collision-free lifetime of a high rotational level ($N' = 30$), excited via the $R_{11}(29)/R_{33}(29)$ lines, to be 32 ± 2 ns. This result is consistent with the findings, reported by Stuart et al., that the lifetimes of $v' = 1$ are independent of rotational levels. In contrast to the $v' = 1$ case, Stuart et al. have found that lifetimes of $v' = 2$ are strongly dependent on rotational levels, ranging from 28 to 91 ns. They measured lifetimes of $N' = 21$ ($J' = 20$ and 22) to be 31.3 ns, which agrees with our value (27 ± 4 ns) for the same rotational level.

Quenching Rate Constants of SO($B^3\Sigma^-$, $v' = 0$, 1, and 2) by Collisions with He. The slopes of the regression lines shown in Figure 5 give second-order rate constants for deactivation of vibrational levels of SO($B^3\Sigma^-$) by collisions with He: (6.3 ± 0.3) × 10^{-12}, (3.9 ± 0.2) × 10^{-11}, and (1.3 ± 0.2) × 10^{-10} in units of cm^3 $molecule^{-1}$ s^{-1} for $v' = 0$, 1, and 2, respectively (Table 1). Deactivation rate constants are dependent on vibrational levels, whereas collision-free lifetimes of three vibrational levels are nearly identical. Stuart et al.[12] have measured a quenching rate constant of SO($B^3\Sigma^-$, $v' = 2$) by He to be (1.3 ± 0.3) × 10^{-10} cm^3 $molecule^{-1}$ s^{-1}. They excited a different rotational line $P(16)$ from that used in the present study $R(20)$; nevertheless, their value is in perfect agreement with ours. Deactivation rate constants for $v' = 0$ and 1 are measured for the first time in the present study.

In general, helium is known to be an inefficient quencher of diatomic molecules.[40] However, even the lowest vibrational level of SO($B^3\Sigma^-$) is effectively quenched by He, (6.3 ± 0.3) × 10^{-12} cm^3 $molecule^{-1}$ s^{-1}, and the value is more than 10 times larger than that for quenching of SO($A^3\Pi$, $v' = 0$) by He reported by Lo et al.,[5] (5.3 ± 0.9) × 10^{-13}, and by McAuliffe et al.,[25] (4.0 ± 0.8) × 10^{-13} cm^3 $molecule^{-1}$ s^{-1}. Rate constants for deactivation of $B^3\Sigma^-$($v' = 1$ and 2) are the sum of those for vibrational relaxation and electronic quenching ($k_v + k_Q$). The contribution of vibrational relaxation can be estimated from the observed fluorescence intensity of $v' - 1$, e.g., intensities of the faint peaks seen in Figure 2a, following excitation to v'. We have found that vibrational relaxation by He is not efficient and estimated rate constants for $v' = 1 \rightarrow v' = 0$ and $v' = 2 \rightarrow v' = 1$ to be 7 × 10^{-13} and 1 × 10^{-11} cm^3 $molecule^{-1}$ s^{-1}, respectively. Therefore, contributions of vibrational relaxation to collisional deactivation are about 2% for $v' = 1$ and 8% for $v' = 2$. This is in contrast to the case of SO($A^3\Pi$, $v' = 1$). McAuliffe et al.[25] measured the rate constant of deactivation of SO($A^3\Pi$, $v' = 1$) by He, $k_v + k_Q$, to be (4.2 ± 0.2) × 10^{-12} cm^3 $molecule^{-1}$ s^{-1}. They also determined the rate constant for vibrational relaxation $v' = 1 \rightarrow v' = 0$ of $A^3\Pi$ by He to be k_1 = (4.3 ± 0.3) × 10^{-12} cm^3 $molecule^{-1}$ s^{-1}, indicating that electronic quenching of $A^3\Pi$($v' = 1$) by He is negligibly small compared to vibrational relaxation.

The large quenching rate constants of the $B^3\Sigma^-$ state and their strong dependence on vibrational levels can be explained by collision-induced predissociation via the $C^3\Pi$ state. Clerbaux and Colin[8] have reported N' values of predissociation limit for the vibrational levels of the $B^3\Sigma^-$ state: 65 ($v' = 0$), 53 ($v' = 1$), 37 ($v' = 2$), and 10 ($v' = 3$). The rotational energies of predissociation limits are smaller for higher vibrational levels, and consequently, predissociation is more efficient for higher vibrational levels. Rotational levels $N' = 14-30$ of $v' \leq 2$ are excited in the present study, and they do not predissociate; however, rotational relaxation by collisions with He can populate higher rotational levels than the initially prepared levels. Stuart et al.[12] have determined the rate constant of rotational relaxation by He to be 7.8 × 10^{-10} cm^3 $molecule^{-1}$ s^{-1} from measurement of saturation fluence for an optically pumped SO(B−X) laser. According to this rate constant, a time constant for rotational relaxation at 50 Torr (Figure 3) can be estimated to be 0.8 ns. This is much shorter than both the pulse duration of the excitation laser and fluorescence lifetimes. Therefore, predissociating levels might be populated by rotational relaxation before deactivation. Figure 3 shows that observed time profiles can be well reproduced by convolution (eq 10) using a single decay rate. The deactivation rate constant of a different rotational level ($N' = 30$) of $v' = 1$, (3.6 ± 0.2) × 10^{-11} cm^3 $molecule^{-1}$ s^{-1}, is almost identical with that of $N' = 14$. The findings indicate that rotational motion is thermalized before decay processes.

Quenching from $B^3\Sigma^-$ to $X^3\Sigma^-$ might be inefficient, although the possibility cannot be ruled out. Excitation energies of diatomic radicals, NH($A^3\Pi$, $c^1\Pi$), CH($A^2\Delta$), and OH($A^2\Sigma^+$), are compatible to that of SO($B^3\Sigma^-$). It has been well-known that the hydride radicals are hardly quenched to the ground electronic states by He.[40-42] Therefore, 20 000−30 000 cm^{-1} of electronic energy of SO($B^3\Sigma^-$) are not likely to be transferred to translational motion between SO and He.

Summary

This paper describes radiative lifetimes and deactivation rate constants of SO($B^3\Sigma^-$, $v' = 0$, 1, and 2) by collisions with He. An integrated phase plane method was applied to analyze time profiles of fluorescence, and reliability of derived parameters were confirmed using convolution integral. Radiative lifetimes of SO($B^3\Sigma^-$) have been determined to be (28 ± 2), (30 ± 3), and (27 ± 4) ns for $v' = 0$ ($N' = 16$), 1 ($N' = 14$), and 2 ($N' = 21$), respectively. The present study also gives the first detailed results on deactivation of SO($B^3\Sigma^-$) by He. Rate coefficients for deactivation of SO($B^3\Sigma^-$) by collisions with He have been obtained to be (6.3 ± 0.3) × 10^{-12}, (3.9 ± 0.2) × 10^{-11}, and (1.3 ± 0.2) × 10^{-10} in units of cm^3 $molecule^{-1}$ s^{-1} for $v' = 0$, 1, and 2, respectively. The efficient deactivation even by He and strong vibrational level dependence can be attributed to predissociation by way of the $C^3\Pi$ state.

Acknowledgment. The authors gratefully acknowledge Craig A. Taatjes (Sandia National Laboratory) for fruitful discussion. This work was supported by the Grant-in-Aid for Scientific Research on Priority Areas "Free Radical Science" (Contract No. 05237106), Grant-in-Aid for Scientific Research (B) (Contract No. 08454181), and Grant-in-Aid for Scientific Research (C) (Contract No. 10640486) of the Ministry of Education, Science, Sports, and Culture.

References and Notes

(1) Clyne, M. A. A.; McDermid, I. S. *J. Chem. Soc., Faraday Trans. 2* **1979**, *75*, 905.
(2) Clyne, M. A. A.; Liddy, J. P. *J. Chem. Soc., Faraday Trans. 2* **1982**, *78*, 1127.
(3) Cao, D.-Z.; Setser, D. W. *Chem. Phys. Lett.* **1985**, *116*, 363.
(4) Cao, D.-Z.; Setser, D. W. *J. Phys. Chem.* **1988**, *92*, 1169.
(5) Lo, G.; Beaman, R.; Setser, D. W. *Chem. Phys. Lett.* **1988**, *149*, 384.
(6) Miller, H. C.; Yamasaki, K.; Smedley, J. E.; Leone, S. R. *Chem. Phys. Lett.* **1991**, *181*, 250.
(7) Herzberg, G. *Molecular Spectra and Molecular Structure, IV. Constants of Diatomic Molecules*; Van Nostrand Reinhold: New York, 1979.
(8) Clerbaux, C.; Colin, R. *J. Mol. Spectrosc.* **1994**, *165*, 334.

(9) Clyne, M. A. A.; Tennyson, P. H. *J. Chem. Soc., Faraday Trans. 2* **1986**, *82*, 1315.
(10) Smith, W. H. *J. Quant. Spectrosc. Radiat. Transfer* **1969**, *9*, 1191.
(11) Martin, E. V. *Phys. Rev.* **1932**, *41*, 167.
(12) Stuart, B. C.; Cameron, S. M.; Powell, H. T. *J. Phys. Chem.* **1994**, *98*, 11499.
(13) Demas, J. N. *Excited State Lifetime Measurements*; Academic Press: New York, 1983.
(14) Norrish, R. G. W.; Oldershaw, G. A. *Proc. R. Soc. London A* **1959**, *249*, 498.
(15) Powell, F. X.; Lide, D. R., Jr. *J. Chem. Phys.* **1964**, *41*, 1413.
(16) Colin, R. *Can. J. Phys.* **1969**, *47*, 979.
(17) Kanamori, H.; Butler, J. E.; Kawaguchi, K.; Yamada, C.; Hirota, E. *J. Mol. Spectrosc.* **1985**, *113*, 262.
(18) Smith, W. H. *Astrophys. J.* **1972**, *176*, 265.
(19) Krause, H. F. *Chem. Phys. Lett.* **1981**, *83*, 165.
(20) Colin, R. *J. Chem. Soc., Faraday Trans. 2* **1982**, *78*, 1139.
(21) Wu, K. T.; Morgner, H.; Yencha, A. J. *Chem. Phys.* **1982**, *68*, 285.
(22) Dorthe, G.; Costes, M.; Burdenski, S.; Caille, J.; Caubet, Ph. *Chem. Phys. Lett.* **1983**, *94*, 404.
(23) Johnson, C. A. F.; Kelly, S. D.; Parker, J. E. *J. Chem. Soc., Faraday Trans. 2* **1987**, *83*, 985.
(24) Kulander, K. C. *Chem. Phys. Lett.* **1988**, *149*, 392.
(25) McAuliffe, M. J.; Bohn, M.; Dorko, E. A. *Chem. Phys. Lett.* **1990**, *167*, 27.
(26) Stuart, B. C.; Cameron, S. M.; Powell, H. T. *Chem. Phys. Lett.* **1992**, *191*, 273.
(27) Kanamori, H.; Butler, J. E.; Kawaguchi, K.; Yamada, C.; Hirota, E. *J. Chem. Phys.* **1985**, *83*, 611.
(28) Kolbe, W. F.; Leskovar, B. *J. Chem. Phys.* **1986**, *85*, 7117.
(29) Kawasaki, M.; Sato, H. *Chem. Phys. Lett.* **1987**, *139*, 585.
(30) Felder, P.; Effenhauser, C. S.; Haas, B.-M.; Huber, J. R. *Chem. Phys. Lett.* **1988**, *148*, 417.
(31) Chen, X.; Asmar, F.; Wang, H.; Weiner, B. R. *J. Phys. Chem.* **1991**, *95*, 6415.
(32) Felder, P.; Haas, B.-M.; Huber, J. R. *Chem. Phys. Lett.* **1993**, *204*, 248.
(33) Hui, M. H.; Rice, S. A. *Chem. Phys. Lett.* **1972**, *17*, 474.
(34) Kanamori, H.; Tiemann, E.; Hirota, E. *J. Chem. Phys.* **1988**, *89*, 621.
(35) Okabe, H. *Photochemistry of Small Molecules*; Wiley: New York, 1978.
(36) Calvert, J. G.; Pitts, J. N., Jr. *Photochemistry*; John Wiley and Sons: New York, 1966.
(37) Okabe, H. *J. Am. Chem. Soc.* **1971**, *93*, 7095.
(38) Smith, W. H.; Liszt, H. S. *J. Quant. Spectrosc. Radiat. Transfer* **1971**, *11*, 45.
(39) Hébert, G. R.; Hodder, R. V. *J. Phys. B* **1974**, *7*, 2244.
(40) Kenner, R. D.; Rohrer, F.; Stuhl, F. *J. Phys. Chem.* **1989**, *93*, 7824.
(41) Hofzumahaus, A.; Stuhl, F. *J. Chem. Phys.* **1985**, *82*, 3152.
(42) Crosley, D. R. *J. Phys. Chem.* **1989**, *93*, 6273.